

Model Independent Dark Matter Properties from Cosmic Growth

Tilek Zhumabek^{1,2}, Mikhail Denissenya¹, Eric V. Linder^{1,3}

¹*Energetic Cosmos Laboratory, Nazarbayev University, Astana 010000, Qazaqstan*

²*Department of Physics, School of Sciences and Humanities, Nazarbayev University, Astana 010000, Qazaqstan*

³*Berkeley Center for Cosmological Physics & Berkeley Lab, University of California, Berkeley, CA 94720, USA*

(Dated: November 29, 2023)

Dark matter dominates the matter budget of the universe but its nature is unknown. Deviations from the standard model, where dark matter clusters with the same gravitational strength as baryons, and has the same pressureless equation of state as baryons, can be tested by cosmic growth measurements. We take a model independent approach, allowing deviations in bins of redshift, and compute the constraints enabled by ongoing cosmic structure surveys through redshift space distortions and peculiar velocities. These can produce constraints at the 3–14% level in four independent redshift bins over $z = [0, 4]$.

I. INTRODUCTION

Dark matter is an essential ingredient of the standard model of cosmology [1–3] and critical to explaining the formation of cosmic structure and the properties of galaxies [4]. Indeed, dark matter contributes ~ 6 times more than standard model baryonic matter to the energy budget of the universe. However, the properties of dark matter, even as it relates to their cosmological effects, are not clearly known.

A plethora of dark matter cosmic properties have been postulated, often to address apparent tensions in galaxy structure or cosmological parameter determination. These include nonstandard interactions, decays, cannibalism, equation of state, etc. A few recent examples include [5–9]. One can also take a more phenomenological point of view, often called “generalized dark matter” [10], where an equation of state away from the standard pressureless one is allowed, along with a sound speed for the fluid perturbations and a possible viscous sound speed. A few recent examples include [11–13].

In this work we focus on what cosmic growth observations can say about the two properties that we know dark matter possesses: energy density evolution (or equivalently equation of state) and clustering strength (i.e. gravitational or other). That is, how can cosmic data constrain whether dark matter is indeed standard: pressureless (equation of state with $w_{\text{dm}} = 0$) and clustering with gravitational strength ($G = G_N$). In order to be as model independent as possible, we will not adopt functional forms but rather allow independent values in bins of redshift.

In Section II we review the growth equation of linear, subhorizon density perturbations and identify two areas in which it may deviate from the standard model. Section III evaluates the case where the gravitational clustering strength of dark matter is modified, while Section IV investigates when the density evolution (equation of state) of dark matter is modified. In each case, we project constraints from the combinations of galaxy redshift surveys. We conclude in Section V.

II. DARK MATTER AND COSMIC GROWTH

Cosmic structure probes not only the expansion rate of the universe, including the energy density evolution (equation of state) of each component, but the strength with which each cluster, either gravitationally or through interactions or self interactions. Therefore it is a powerful cosmic probe beyond the standard model. Here we will focus on dark matter properties, in a flat universe with baryons, dark matter, and a cosmological constant, with no conversion between them.

In the subhorizon, linear density perturbation regime, matter grows in the standard cosmological model according to

$$\frac{d^2\delta(t)}{dt^2} + 2H(t)\frac{d\delta(t)}{dt} - 4\pi G_N\rho_m(t)\delta(t) = 0, \quad (1)$$

where $\delta = \delta\rho_m/\rho_m$ is the matter overdensity, $\rho_m = \rho_b + \rho_{\text{dm}}$ is the sum of the baryonic matter and dark matter, t is the cosmic time, $H = \dot{a}/a$ is the Hubble parameter, and G_N is the Newton’s constant.

One can of course consider cosmologies other than dark energy being a cosmological constant, in which case H changes (and dark energy perturbations arise, but these generally have negligible impact on matter growth). Instead we keep the dark energy sector as a cosmological constant and explore the dark matter sector, by allowing the dark matter clustering strength to deviate from the universal gravitational strength,

$$G_N\rho_m\delta \rightarrow G_N(\rho_b\delta_b + F_{\text{cl}}\rho_{\text{dm}}\delta_{\text{dm}}). \quad (2)$$

The clustering strength F_{cl} is treated phenomenologically, without a specific model assumed, but time dependence is allowed. This will give a model independent generalization of some investigations in [14]. Such a standard model extension is explored in Section III.

The second modification considered to the standard model is to allow deviations to the dark matter density evolution,

$$\begin{aligned} \rho_{\text{dm}}(a) &= \rho_{\text{dm}}(a=1)a^{-3} \\ &\rightarrow \rho_{\text{dm}}(a=1)a^{-3}F_{\text{eos}}(a). \end{aligned} \quad (3)$$

Again we treat F_{eos} phenomenologically. This will change $H(t)$ as well as the source term of the growth evolution equation. If one altered dark energy as well to preserve $H(t)$, this approach becomes equivalent to a change F_{cl} entering just the source term, so we keep dark energy fixed as a cosmological constant. This extension is explored in Section IV.

In both cases we adopt a model independent approach by fitting the deviating functions F in independent bins of redshift. We fix the baryons to have standard evolution $\rho_b \sim a^{-3}$, with value today $\Omega_{b,0} h^2 = 0.02233$ indicated by primordial nucleosynthesis and cosmic microwave background (CMB) measurements. We also take $h = 0.7$ ($\Omega_b = 0.0456$) and a fiducial $\Omega_{m,0}^{\text{LCDM}} = 0.3$.

III. DARK MATTER CLUSTERING

Galaxy redshift surveys map large scale structure over a redshift range, and the clustering evolution depends not only on the growth factor $\delta(t)$ but on the growth rate $f = d \ln \delta / H dt = d \ln \delta / d \ln a$ entering into redshift space distortions (RSD). It is convenient to work in terms of scale factor a or redshift $z = a^{-1} - 1$, and also to normalize the growth factor to take out the matter dominated behavior $\delta^{\text{md}} \sim a$ by using $g(a) = [\delta(a)/\delta(a_i)]/(a/a_i)$, where a_i is some initial condition scale factor in the matter dominated epoch (where $g = 1$, $f = 1$).

The growth evolution equation can then be written as

$$0 = a^2 \frac{d^2 g}{da^2} + \left(5 + \frac{1}{2} \frac{d \ln H^2}{d \ln a} \right) a \frac{dg}{da} + \left(3 + \frac{1}{2} \frac{d \ln H^2}{d \ln a} - \frac{3}{2} [\Omega_b(a) + F_{\text{cl}}(a) \Omega_{\text{dm}}(a)] \right) g. \quad (4)$$

Note that $f = 1 + d \ln g / d \ln a$ and that RSD involves $f \sigma_8(a)$ where $\sigma_8(a) \sim \delta$ is related to the mass fluctuation amplitude (so $f \sigma_8 \sim d \delta / d \ln a$). While one could fix the value of σ_8 at present as measured by mass clustering, we want to keep the high redshift universe within the standard cosmological model and so normalize in terms of the CMB fluctuation amplitude quantity A_s . Deviations in clustering strength (or in dark matter density evolution in the next section) will therefore alter the value of $\sigma_{8,0}$. We can write

$$f \sigma_8(a) = \frac{\sigma_{8,0}^{\text{LCDM}}}{g_0^{\text{LCDM}}} a g \left(1 + \frac{d \ln g}{d \ln a} \right). \quad (5)$$

For our fiducial model, $g_0^{\text{LCDM}} = 0.779$ and we take $\sigma_{8,0}^{\text{LCDM}} = 0.8$.

A. Sensitivity to Deviations

We first investigate how the quantities $g(a)$ and $f \sigma_8(a)$ respond to deviations in dark matter clustering. For a model independent approach we take

$$F_{\text{cl}}(a) = 1 + c(a), \quad (6)$$

with the deviations c given by bins in scale factor with amplitude c_i . We choose four bins with $a = [0.2, 0.333], [0.333, 0.5], [0.5, 0.667], [0.667, 1]$. For $a < 0.2$ we set the deviation to 0, preserving the high redshift universe and in particular primordial nucleosynthesis and the primary CMB. Then c_1 represents a deviation in the earliest bin and c_4 in the latest bin.

Since growth is a dynamical process we expect the growth at some time to be influenced by the conditions at all earlier times. Thus a tomographic survey covering a broad range of redshifts will be useful in indicating when the deviations arise. Note that F_{cl} can be interpreted as either all the dark matter clustering with strength different from gravitational (G_N), or only some fraction of the dark matter clustering, e.g. if there are multiple species of dark matter.

Figure 1 shows the impact of $c_i = \pm 0.05$ for each bin individually on the growth factor g and RSD factor $f \sigma_8$. The fractional deviation of each quantity from their LCDM values is given in Figure 2. As expected, a change in clustering in the earliest bin has longest, sustained impact on the growth. We can enhance or suppress growth by changing the clustering from the standard model. Note that since we turn on the deviation only for the length of a bin, the effect on the growth rate $f \sigma_8$ begins to diminish at the end of the appropriate bin, but there is an ‘‘inertia’’ in g as it is an integral of $f \sigma_8$.

In order to constrain the deviations with data we will employ the information matrix formalism to determine $\sigma(c_i)$ for various combinations of surveys. The information sensitivity $\partial \mathcal{O} / \partial c_i$ of an observable \mathcal{O} is shown in Figure 3 for g and $f \sigma_8$. We will not actually use g in our constraints due to its degeneracy with galaxy bias, which can also be redshift dependent. This could be lifted using higher order correlation functions or data other than growth, e.g. weak gravitational lensing or the cosmic microwave background, but here we only use as data the RSD factor $f \sigma_8$.

Note that the sensitivity curves are distinct in shape, which generally indicates that covariances between the parameters can be broken by data extending over a broad redshift range. The $f \sigma_8$ sensitivity curves rise linearly at high redshift, reflecting the results of [15] (see, e.g., Fig. 6 there) that the deviation in $f \sigma_8$ is proportional to the area under the curve of the clustering deviation, which grows linearly with scale factor between the bin boundaries. At more recent scale factor the proportionality to area is modified and the sensitivity grows somewhat more slowly than linear. After the more recent bin boundary is reached, $f \sigma_8$ still has an inertia or hysteresis from the deviation and only slowly approaches back to the LCDM behavior.

B. Estimated Constraints on Deviations

Given cosmic survey data we can constrain the clustering deviations allowed through the standard information

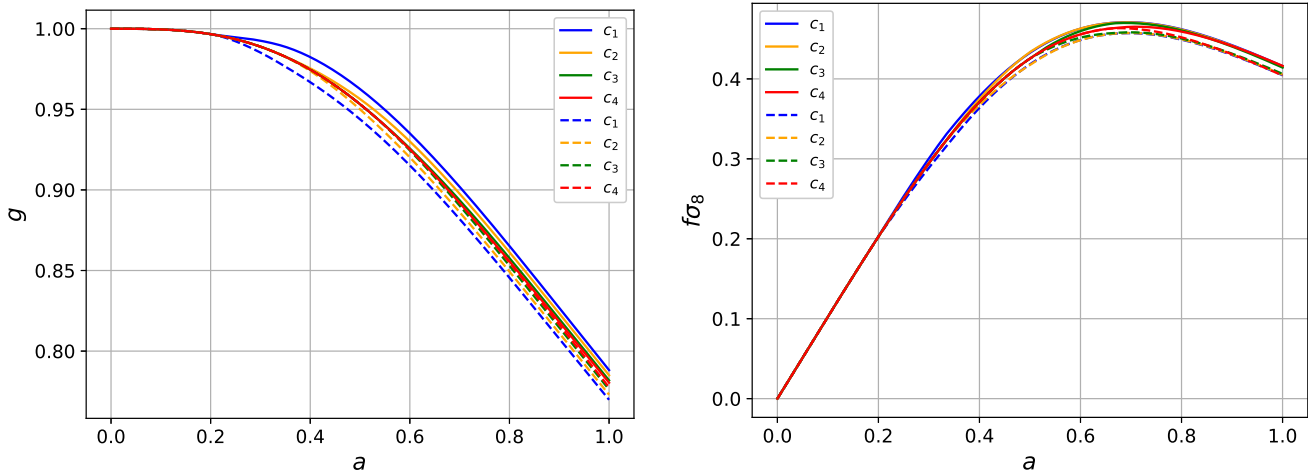


FIG. 1. The growth factor $g(a)$ [left panel] and RSD factor $f\sigma_8(a)$ [right panel] react to the deviation in dark matter clustering behavior. Here each deviation $c_i = \pm 0.05$ (solid/dashed curves respectively) is turned on one at a time.

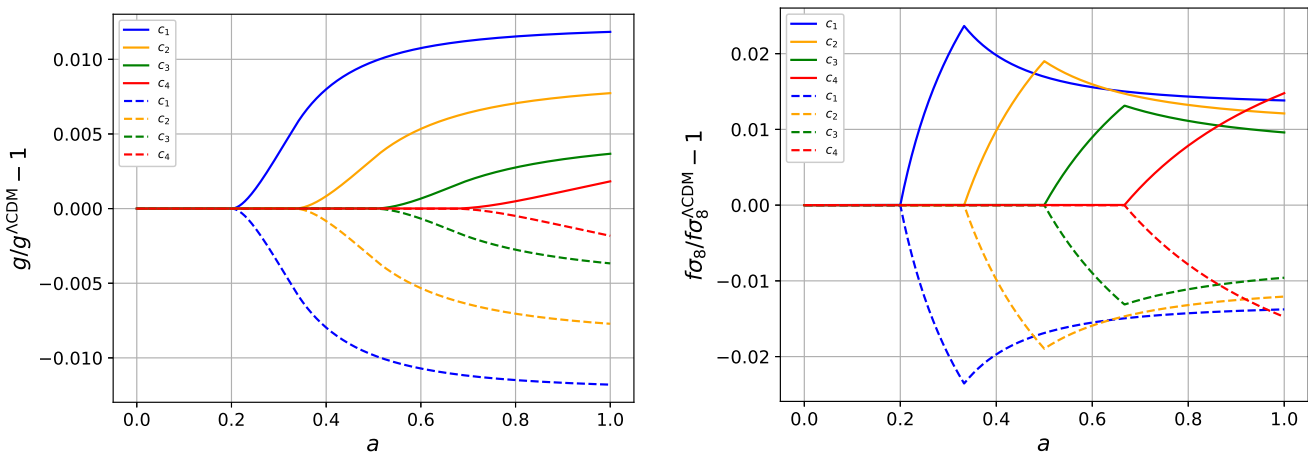


FIG. 2. As in Figure 1 but shown as residuals relative to the LCDM behavior.

matrix formalism. As the binned clustering parameters span a wide range of scale factor, we consider combinations of three different surveys. The mock data will be 2% precision measurements of $f\sigma_8$ from redshift space distortions in independent redshift bins $z = 0.35, 0.45, \dots, 1.55$, denoted as “desi” since it bears similarity to expected measurements from DESI [16], plus measurements at $z = 1.65, 1.75, 1.85, 1.95$, denoted as “euclid” (cf. [17]), plus peculiar velocity measurement of $f\sigma_8$ at $z = 0.1$, denoted “pv”, as might be enabled by DESI [18–20]. We use lower case names to emphasize these are approximate similarities, not meant to capture fully the experiments. The five fit parameters are $\Omega_{m,0}$ and the four c_i , with fiducial values $\Omega_{m,0} = 0.3$, $c_i = 0$. We also add a Gaussian prior $\sigma_{\Omega_{m,0}} = 0.02$ to represent information from external data, e.g. supernova and baryon acoustic oscillation distances.

Figure 4 illustrates the results for three combinations of data. Constraints on c_1 , in the highest red-

shift bin, are strongly helped by the addition of euclid data, while constraints on c_4 , in the lowest redshift bin, benefit from pv data. When using all three data sets, the clustering deviations are estimated to $\sigma(c_i) = (0.0282, 0.0524, 0.0888, 0.1367)$ respectively. The binned values are fairly independent of each other, with their strongest correlation being $r(c_2, c_4) = 0.49$.

IV. DARK MATTER EQUATION OF STATE

Changing the evolution of the dark matter density influences both the source term and the background expansion in the growth equation. The density evolution can be phrased in terms of the dark energy equation of state parameter w_{dm} . We allow this to vary independently in the same four scale factor bins as before, with again the standard behavior $w_{\text{dm}} = 0$ for $a < 0.2$. The clustering

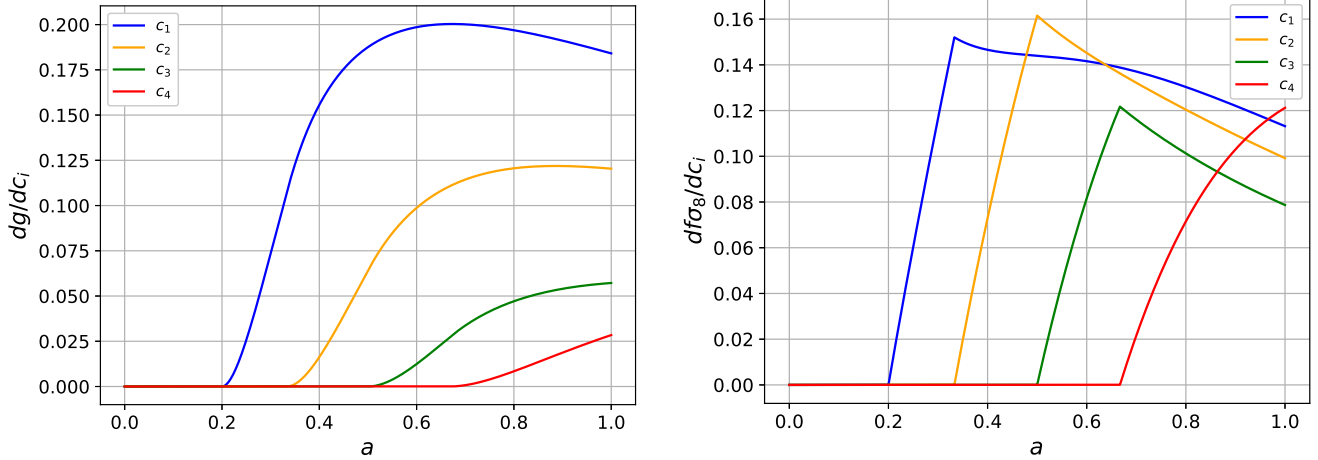


FIG. 3. Information sensitivity plots of the growth factor g and RSD factor $f\sigma_8$. Since the reactions with respect to the clustering strength parameters c_i have different shapes, data over a wide range of redshifts can ameliorate covariances between them.

strength is kept at the standard gravitational coupling G_N in this section.

(This basically follows the generalized dark matter paradigm of [10], where the dark matter properties are described by $w_{\text{dm}}(a)$, the general sound speed $c_s(a)$, and the viscous sound speed $c_{\text{vis}}(a)$. To focus on the influence of changes in the dark matter density evolution, we fix c_s and c_{vis} to their standard values of zero. In any case, [21–25] demonstrated their effects to be small generally.)

Since the density evolution is related to the equation of state by

$$\rho_{\text{dm}} = \rho_{\text{dm}}(a=1) e^{3 \int_a^1 (da'/a') [1+w(a')]} , \quad (7)$$

then we see that from Eq. (3)

$$\rho_{\text{dm}}(a) = \rho_{\text{dm}}^{\text{LCDM}}(a=1) a^{-3} \prod_{i=1}^j \left(\frac{\min[a, a_{i+1}]}{a_i} \right)^{-3w_i} , \quad (8)$$

where the upper limit j denotes the bin in which a is evaluated (e.g. $j=1$ if $a_1 < a < a_2$, and $a_5 > 1$ so $j=4$ for $a_4 < a \leq 1$). For $a < a_1$ then the product is taken to be 1, and so $\rho_{\text{dm}}(a < a_1) = \rho_{\text{dm}}^{\text{LCDM}}(a < a_1)$, i.e. the high redshift behavior is unaffected, as desired. Since we keep h (i.e. H_0) fixed, then

$$\Omega_{\text{dm},0} = \Omega_{\text{dm},0}^{\text{LCDM}} a_1^{3w_1} a_2^{3(w_2-w_1)} a_3^{3(w_3-w_2)} a_4^{3(w_4-w_3)} . \quad (9)$$

As usual $\Omega_{m,0} = \Omega_{b,0} + \Omega_{\text{dm},0}$; note that when $w_i \neq 0$ then $\Omega_{m,0} \neq \Omega_{m,0}^{\text{LCDM}}$. When all $w_i = 0$ then the expressions restore to the standard cosmology.

The growth factor g and RSD factor $f\sigma_8$ are plotted in Figure 5 for individual deviations $w_i = \pm 0.05$. We note that there is actually a crossing of the LCDM behavior in each curve. This is clearer in Figure 6 that shows the residuals with respect to LCDM. Here there are three stages to the deviations in growth. Although in

the matter dominated epoch before the first redshift bin for equation of state deviation w_i , the model is LCDM, it is not the *same* LCDM model as the fiducial because $\Omega_{\text{dm},0} \neq \Omega_{\text{dm},0}^{\text{LCDM}}$ as seen from Eq. (9). In particular, at high redshift before the first bin, Eqs. (8) and (9) give

$$H^2(a < a_1)/H_0^2 = \Omega_{m,0}^{\text{LCDM}} a^{-3} + 1 - \Omega_{b,0} - \Omega_{\text{dm},0} , \quad (10)$$

so the cosmological constant term is offset. Only when all $w_i = 0$ does $\Omega_{\text{dm},0}$ and $H^2(a < a_1)$ fully restore to the fiducial.

Since $H^2(a < a_1)$ differs from the fiducial LCDM, as a^3 (so by very little at high redshift), the growth will actually be affected by a small amount even before the first bin. From Eq. (7) in [26], it is straightforward to calculate that this implies that the growth rate f (and hence the growth factor g) deviates from the fiducial as a^3 . Since $\Omega_{\text{dm},0}$ decreases as w_i increases, this suppresses growth for positive w_i . This defines the first stage (pre-bin) in the fractional deviations shown in Figure 6. The next stage occurs within the bin where w_i deviates from zero. Here, the friction term in the growth equation is suppressed (enhanced) and the growth increases (decreases) for positive (negative) w_i . Recall that $d \ln H^2 / d \ln a = -3(1 + w_{\text{tot}})$ and increasing the dark matter equation of state parameter increases the total equation of state w_{tot} . Finally, after the bin deviation is turned off, again the reduced $\Omega_{\text{dm},0}$ suppresses growth, though more modestly than at the a^3 rate in the matter dominated era.

The sensitivity derivatives plotted in Figure 7 again show these three physical behaviors. However now, as with the clustering deviations, an equation of state deviation in a bin has an inertial effect on the growth, persisting somewhat after the deviation turns off until the reduced $\Omega_{\text{dm},0}$ takes over.

The fit parameters in this section are $\Omega_{m,0}^{\text{LCDM}}$ and the four w_i , with fiducial values $\Omega_{m,0}^{\text{LCDM}} = 0.3$ and $w_i = 0$.

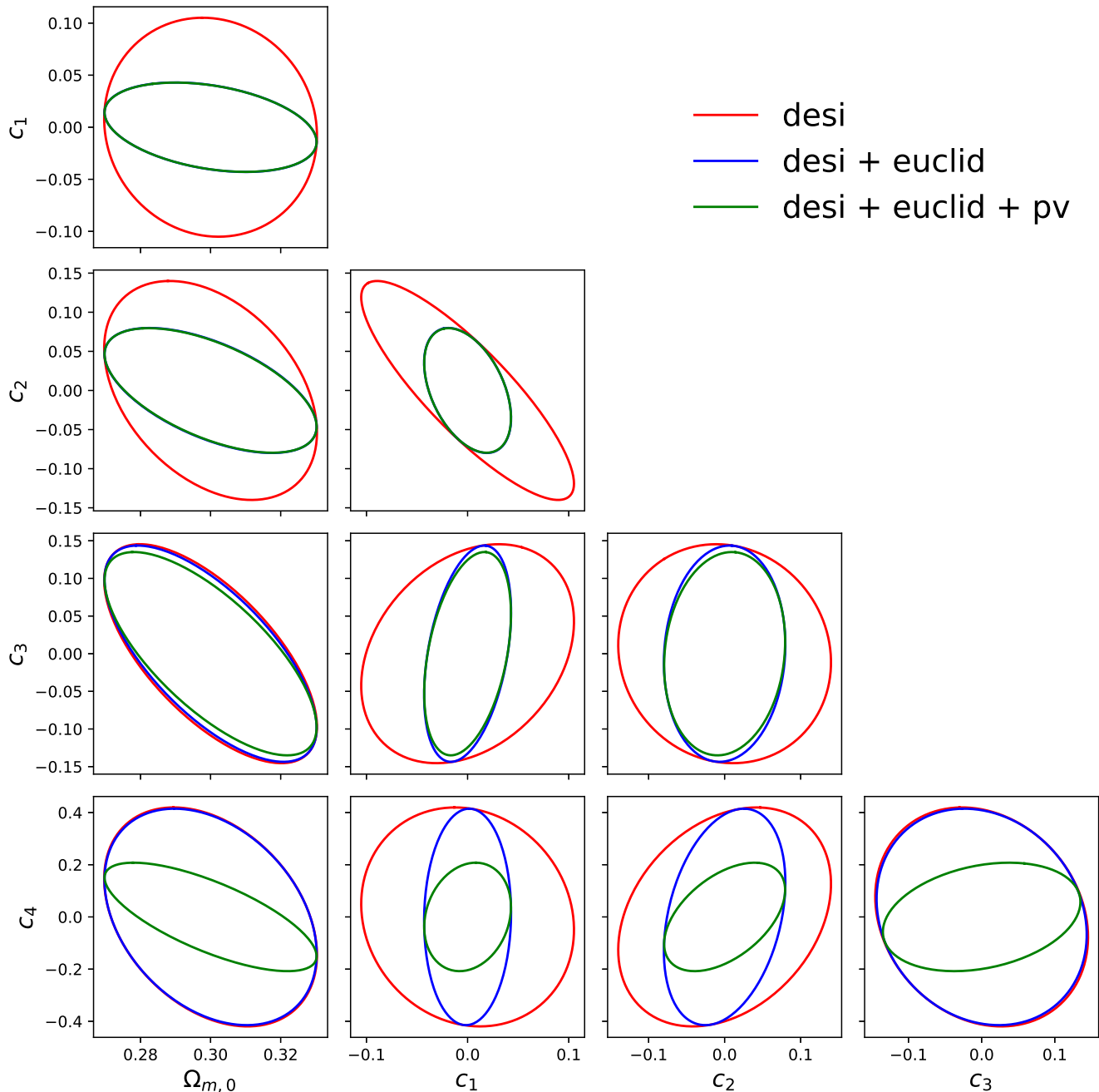


FIG. 4. 68% joint confidence level contours on the dark matter clustering parameters and matter density for various data combinations. “desi” indicates 2% precision on $f\sigma_8$ from $z = [0.3, 1.6]$, with “euclid” adding the range $z = [1.6, 2]$, and “pv” adding peculiar velocity measurement of $f\sigma_8$ to 2% at $z = 0.1$. All cases have a prior $\sigma_{\Omega_{m,0}} = 0.02$.

We expect somewhat more covariance among the parameters than previously due to their appearance in $\Omega_{\text{dm},0}$, Eq. (9).

Using the same combinations of data sets as previously, Figure 8 presents the 2D joint confidence contours for the parameter constraints. When using all three data sets, with the matter density prior, the dark matter equation of state deviations are limited to $\sigma(w_i) =$

$(0.0300, 0.0497, 0.0926, 0.2293)$ respectively. The binned values are fairly independent of each other, with their strongest correlation being $r(w_1, w_2) = -0.75$.

Note that the impact of the low redshift peculiar velocity measurement is weaker in this case, especially on w_4 . This is due to two factors: as seen in Figure 7 the sensitivity of $f\sigma_8$ at low redshift directly to w_4 is smaller than to the other w_i (compare Fig. 3), and the covariance

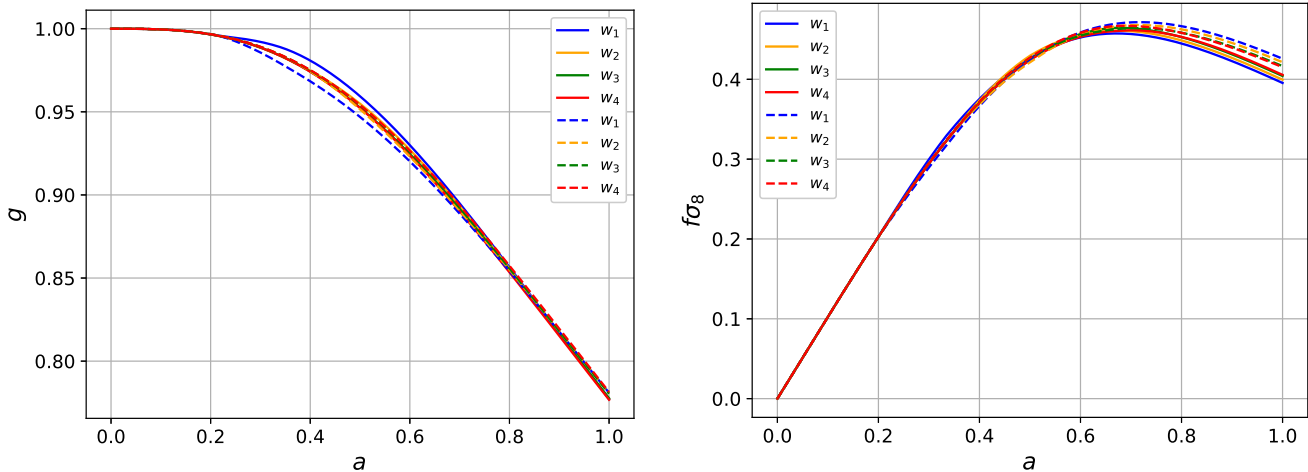


FIG. 5. The growth factor $g(a)$ [left panel] and RSD factor $f\sigma_8(a)$ [right panel] react to the deviation in dark matter equation of state. Here each deviation $w_i = \pm 0.05$ (solid/dashed curves respectively) is turned on one at a time.

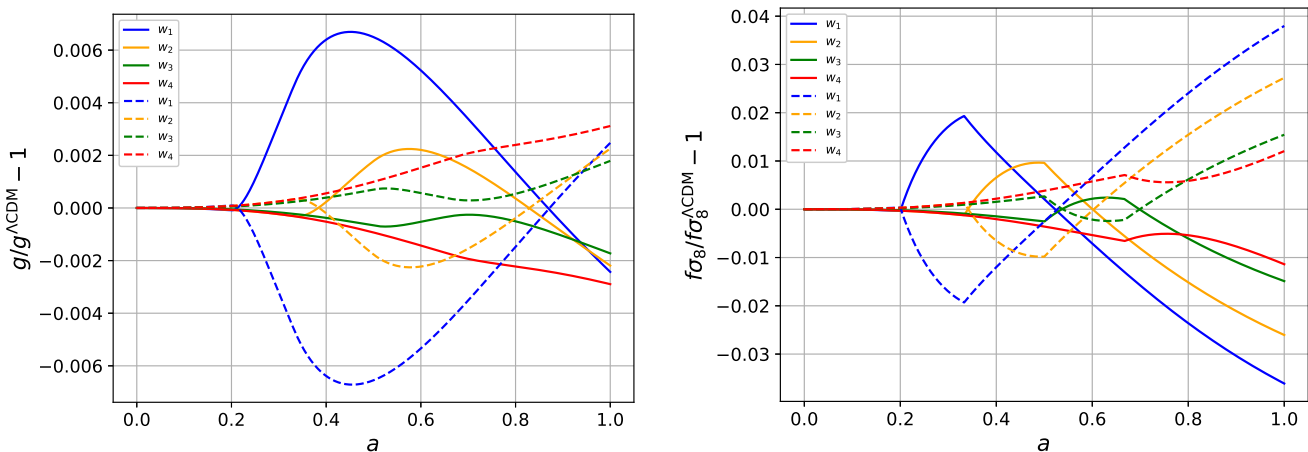


FIG. 6. As in Figure 5 but shown as residuals relative to the fiducial LCDM behavior.

between w_4 and $\Omega_{\text{dm},0}$ is much higher, with correlation coefficient $r(w_4, \Omega_{\text{dm},0}) = 0.95$, reducing the constraining power of the low redshift measurement. The peculiar velocity measurement does help with the next lower bin, w_3 . Adding high redshift measurements improves the higher redshift bins, i.e. constraints on w_1 and w_2 .

V. CONCLUSIONS

Dark matter is prevalent on cosmic scales but apart from its density we have relatively little idea about its properties. Here we examined two characteristics – its clustering strength and equation of state. Our approach emphasized model independence, with independent bins in redshift.

We first test whether dark matter clusters with gravitational strength. Cosmic growth of structure is an excel-

lent probe for this, and we find a strong complementarity between surveys covering a diversity of redshift ranges. Redshift space distortion measurements of a precision similar to Euclid and DESI, and low redshift peculiar velocity measurement as could be enabled by DESI and other experiments, can constrain the clustering strength at the 3–14% level over the four independent redshift bins. This could be tightened by using fewer bins to look for a deviation signal, then fine tuning the bins to characterize it.

The second investigation considers constraints on deviation of the dark matter equation of state from zero, i.e. $\rho_{\text{dm}} \approx a^{-3}$. Here the constraints on the four binned values are at the $\sigma(w_i) = 0.03 - 0.23$ level. This limits how much dark matter can deviate from pressureless behavior.

One can of course obtain tighter constraints in both cases by adopting a specific functional form for the deviation behavior, but given the uncertainty about the

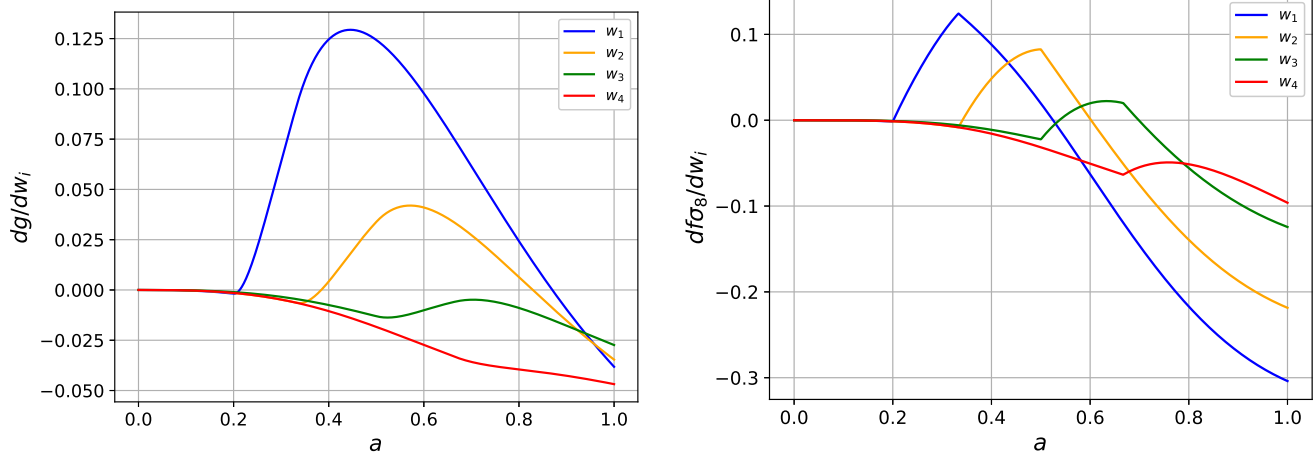


FIG. 7. Sensitivity of growth factor g [left panel] and RSD factor $f\sigma_8$ [right panel] to the dark matter equation of state parameters w_i .

dark matter sector we prefer the model independent approach. Future surveys to even higher redshift, such as MegaMapper [27] or Spec-S5 [28], could also improve constraints, adding to their science cases for dark energy [29, 30]. Further dark matter properties such as its (non-adiabatic) sound speed and viscous sound speed could be constrained in a similar model independent manner; we leave this for future work.

ACKNOWLEDGMENTS

This work was supported in part by the Energetic Cosmos Laboratory. EL is supported in part by the U.S. Department of Energy, Office of Science, Office of High Energy Physics, under contract number DE-AC02-05CH11231.

-
- [1] D. Clowe, M. Bradač, A. H. Gonzalez, M. Markevitch, S. W. Randall, C. Jones, and D. Zaritsky, A direct empirical proof of the existence of dark matter, *The Astrophysical Journal* **648**, L109–L113 (2006), [arXiv:astro-ph/0608407](https://arxiv.org/abs/astro-ph/0608407).
- [2] N. Aghanim *et al.*, Planck 2018 results: VI. cosmological parameters, *Astronomy and Astrophysics* **641**, A6 (2020), [arXiv:1807.06209](https://arxiv.org/abs/1807.06209) [astro-ph.CO].
- [3] L. Baudis and S. Profumo, Dark Matter in R. L. Workman *et al.*, (Particle Data Group), Review of Particle Physics, *PTEP* **2022**, 083C01 (2022), <https://pdg.lbl.gov/2023/reviews/rpp2022-rev-dark-matter.pdf>.
- [4] R. H. Wechsler and J. L. Tinker, The connection between galaxies and their dark matter halos, *Annual Review of Astronomy and Astrophysics* **56**, 435–487 (2018), [arXiv:1804.03097](https://arxiv.org/abs/1804.03097) [astro-ph.CO].
- [5] E. Di Valentino, O. Mena, S. Pan, L. Visinelli, W. Yang, A. Melchiorri, D. F. Mota, A. G. Riess, and J. Silk, In the realm of the hubble tension—a review of solutions, *Classical and Quantum Gravity* **38**, 153001 (2021), [arXiv:2103.01183](https://arxiv.org/abs/2103.01183) [astro-ph.CO].
- [6] A. Ashoorioon and Z. Davari, Dark matter cosmology with varying viscosity: a possible resolution to the S_8 tension, [arXiv:2303.06627](https://arxiv.org/abs/2303.06627) [astro-ph.CO].
- [7] P. Arabameri, Z. Davari, and N. Khosravi, k -dependent dark matter, [arXiv:2307.08495](https://arxiv.org/abs/2307.08495) [hep-ph].
- [8] K. Naidoo, Signs of a non-zero equation-of-state for dark matter, [arXiv:2308.13617](https://arxiv.org/abs/2308.13617) [astro-ph.CO].
- [9] A. Lapi, L. Boco, M. M. Cueli, B. S. Haridasu, T. Ronconi, C. Baccigalupi, and L. Danese, Little ado about everything: η CDM, a cosmological model with fluctuation-driven acceleration at late times, [arXiv:2310.06028](https://arxiv.org/abs/2310.06028) [astro-ph.CO].
- [10] W. Hu, Structure formation with generalized dark matter, *The Astrophysical Journal* **506**, 485–494 (1998), [arXiv:astro-ph/9801234](https://arxiv.org/abs/astro-ph/9801234).
- [11] K. Naidoo, M. Jaber, W. A. Hellwing, and M. Bilicki, A dark matter solution to the H_0 and S_8 tensions, and the integrated Sachs-Wolfe void anomaly (2023), [arXiv:2209.08102](https://arxiv.org/abs/2209.08102) [astro-ph.CO].
- [12] V. Yadav, S. K. Yadav, and A. K. Yadav, Observational constraints on generalized dark matter properties in the presence of neutrinos with the final Planck release, [arXiv:2307.05155](https://arxiv.org/abs/2307.05155) [astro-ph.CO].
- [13] M. Meiers, L. Knox, and N. Schöneberg, Exploration of the pre-recombination universe with a high-dimensional model of an additional dark fluid, [arXiv:2307.09522](https://arxiv.org/abs/2307.09522) [astro-ph.CO].
- [14] E. V. Linder, Testing dark matter clustering with redshift space distortions, *Journal of Cosmology and Astroparticle Physics* **2013** (04), 031, [arXiv:1302.4754](https://arxiv.org/abs/1302.4754) [astro-ph.CO].
- [15] M. Denissenya and E. V. Linder, Cosmic growth signatures of modified gravitational strength, *Journal of Cosmology and Astroparticle Physics* **2017** (06), 030, [arXiv:1703.00917](https://arxiv.org/abs/1703.00917) [astro-ph.CO].

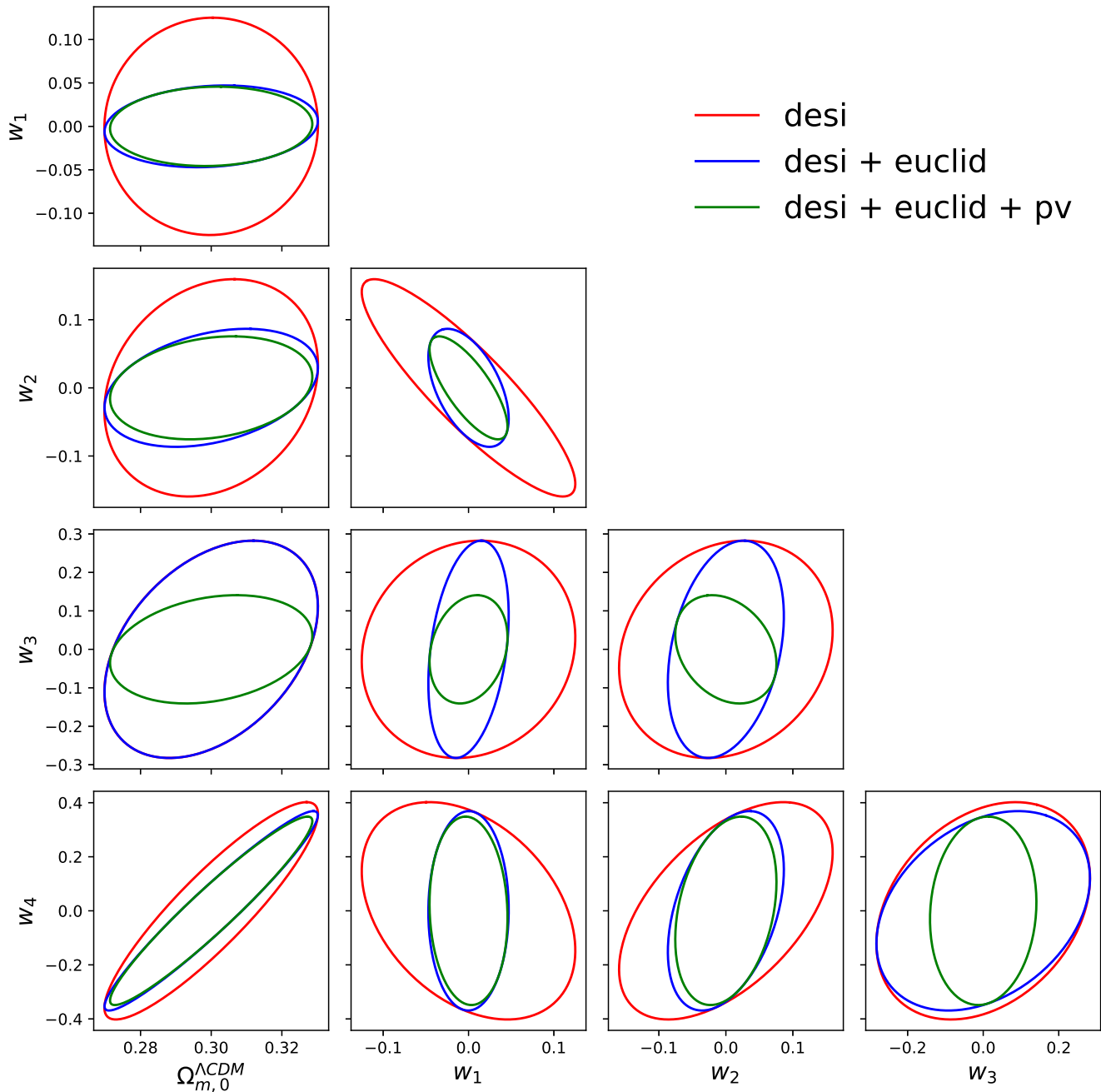


FIG. 8. 68% joint confidence level contours on the dark matter equation of state parameters and matter density for various data combinations. All cases have a prior $\sigma_{\Omega_{m,0}} = 0.02$.

- [16] DESI Collaboration, A. Aghamousa, *et al.*, The DESI experiment part I: science, targeting, and survey design, [arXiv:1611.00036 \[astro-ph.IM\]](#).
- [17] Euclid Collaboration *et al.*, Euclid preparation: VII. forecast validation for Euclid cosmological probes, *Astronomy and Astrophysics* **642**, A191 (2020), [arXiv:1910.09273 \[astro-ph.CO\]](#).
- [18] A. G. Kim and E. V. Linder, Complementarity of peculiar velocity surveys and redshift space distortions for testing gravity, *Physical Review D* **101**, 023516 (2020), [arXiv:1911.09121 \[astro-ph.CO\]](#).
- [19] A. Palmese and A. G. Kim, Probing gravity and growth of structure with gravitational waves and galaxies' peculiar velocity, *Physical Review D* **103**, 103507 (2021), [arXiv:2005.04325 \[astro-ph.CO\]](#).
- [20] C. Saulder *et al.*, Target selection for the DESI peculiar velocity survey, *Monthly Notices of the Royal Astronomical Society* **525**, 1106–1125 (2023), [arXiv:2302.13760 \[astro-ph.CO\]](#).

- [21] C. M. Müller, Cosmological bounds on the equation of state of dark matter, *Physical Review D* **71**, 047302 (2005), [arXiv:astro-ph/0410621](#).
- [22] C. Armendariz-Picon and J. T. Neelakanta, How cold is cold dark matter?, *Journal of Cosmology and Astroparticle Physics* **2014** (03), 049, [arXiv:1309.6971 \[astro-ph.CO\]](#).
- [23] D. B. Thomas, M. Kopp, and C. Skordis, Constraining the properties of dark matter with observations of the cosmic microwave background, *The Astrophysical Journal* **830**, 155 (2016), [arXiv:1601.05097 \[astro-ph.CO\]](#).
- [24] M. Kopp, C. Skordis, D. B. Thomas, and S. Ilić, Dark matter equation of state through cosmic history, *Physical Review Letters* **120**, 221102 (2018), [arXiv:1802.09541 \[astro-ph.CO\]](#).
- [25] S. Ilić, M. Kopp, C. Skordis, and D. B. Thomas, Dark matter properties through cosmic history, *Physical Review D* **104**, 043520 (2021), [arXiv:2004.09572 \[astro-ph.CO\]](#).
- [26] E. V. Linder and R. N. Cahn, Parameterized beyond-Einstein growth, *Astroparticle Physics* **28**, 481–488 (2007), [arXiv:astro-ph/0701317](#).
- [27] D. J. Schlegel *et al.*, The MegaMapper: a stage-5 spectroscopic instrument concept for the study of inflation and dark energy, [arXiv:2209.04322 \[astro-ph.IM\]](#).
- [28] D. J. Schlegel *et al.* (DESI), A spectroscopic road map for cosmic frontier: DESI, DESI-II, stage-5, [arXiv:2209.03585 \[astro-ph.CO\]](#).
- [29] E. V. Linder, The rise of dark energy, [arXiv:2106.09581 \[astro-ph.CO\]](#).
- [30] N. Sailer, E. Castorina, S. Ferraro, and M. White, Cosmology at high redshift - a probe of fundamental physics, *Journal of Cosmology and Astroparticle Physics* **2021** (12), 049, [arXiv:2106.09713 \[astro-ph.CO\]](#).